

Multiview Graph Contrastive Representation Learning for Drug-Drug Interaction Prediction

Yingheng Wang^{1,2}, Yaosen Min³, Xin Chen⁴, Ji Wu¹

¹Department of Electronic Engineering, Tsinghua University

²Department of Biomedical Engineering, Johns Hopkins University

³Institute of Interdisciplinary Information Sciences, Tsinghua University

⁴Technology and Engineering Group, Tencent

wangyh20@mails.tsinghua.edu.cn, minys18@mails.tsinghua.edu.cn,
marcuschen@tencent.com, wuji_ee@mail.tsinghua.edu.cn

Abstract

Drug-drug interaction (DDI) prediction is an important task in the medical health machine learning community. This study presents a new method, Multiview gRaph Contrastive representation Learning for drug-drug interaction prediction, MIRACLE for brevity, to capture inter-view molecule structure and intra-view interactions between molecules simultaneously. MIRACLE treats a DDI network as a multi-view graph where each node in the interaction graph itself is a drug molecular graph instance. We use GCNs and bond-aware attentive message passing networks to encode DDI relationships and drug molecular graphs in the MIRACLE learning stage, respectively. Also, we propose a novel unsupervised contrastive learning component to balance and integrate the multi-view information. Comprehensive experiments on multiple real datasets show that MIRACLE outperforms the state-of-the-art DDI prediction models consistently.

Introduction

Recent progress in machine learning algorithms facilitates the computer-assisted DDI prediction. Although these methods achieve satisfactory results and become state-of-the-art, they still have some limitations. *Firstly*, previous models based on multiple similarity-based fingerprints require feature engineering, which is time-consuming and challenging to collect (Xin, Xien, and Ji 2020). They mainly rely on the empirical assumption that chemically, biologically, or topologically similar drugs are more likely to interact with each other. However, plenty of interacting drug pairs whose pairwise similarities are extremely low may be led to wrong prediction results. Meanwhile, large-scale datasets may be missing some of these features, which are crucial to DDI prediction but unavailable for most kinds of drugs. Therefore, these models **have a deficiency in scalability and robustness**. *Secondly*, in practice, the inter-view information included in the drug molecular graph and the intra-view DDI relationships are both important for the DDI prediction task. The inter-view information contains not only atom and bond features but also structure information inside drug molecules. Besides, the interaction patterns are hidden in

the intra-view DDI relationships. However, previous graph-based works only concentrate on a single view of drugs (Sun et al. 2020). Thus, **the combination of multi-views information inside the DDI network is often overlooked by these methods**.

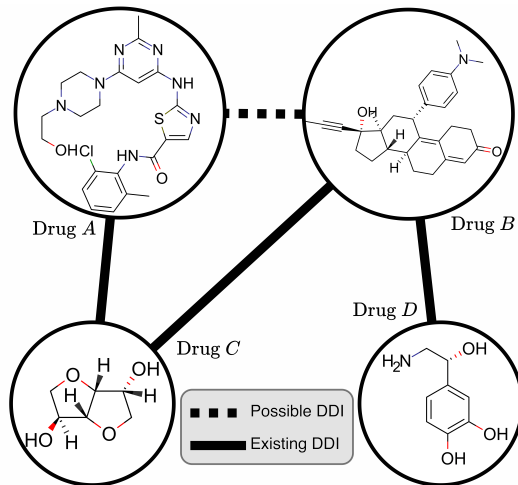


Figure 1: A toy example of the multi-view graph. Drug A, B, C, D denote four drugs in the DDI network. The solid and dashed lines indicate existing and possible interactions. The internal structure of each drug shows its molecular graph.

To overcome the limitations mentioned above, we proposed a novel method, Multiview gRaph Contrastive representation Learning for drug-drug interaction prediction, MIRACLE for brevity, to explore rich multi-views information among drugs and generate accurate latent vectors of drugs. In such a multi-view graph setting, we treat each drug instance as a molecular graph and DDI relationships as an interaction graph, namely the inter- and intra-view, respectively. In the inter-view, we first encode drug molecular graphs into drug embeddings by a bond-aware message passing network fusing information from atom and bond features and molecule structures. Then, we integrate them with the intra-view information, the external DDI relationships to update drug embedding. Also, for the multi-view information integrated into drug embeddings, it is necessary

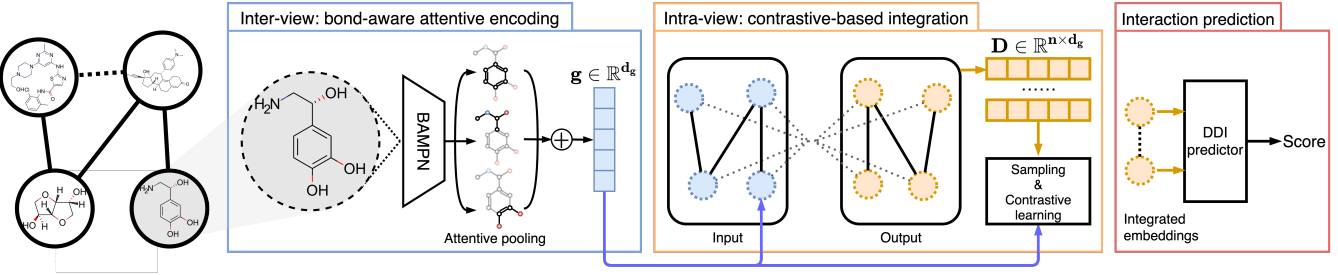


Figure 2: The illustrative schematic diagram of our proposed framework MIRACLE. There are three sequential and interdependent phases: 1) In the inter-view, drug molecular graphs are encoded into drug embeddings by a bond-aware message passing network with attentive pooling. 2) In the intra-view, a GCN encoder is used to integrate the external DDI relationships into drug embeddings. Also, a contrastive learning framework is applied to balance information from different views to update drug embeddings. 3) With the learned drug embeddings, an interaction predictor is designed to generate final prediction results.

to balance information from different views. We use a contrastive learning-based method to tackle this problem. Finally, we obtain interaction embeddings through the learned drug embeddings and make predictions. Figure 1 shows a multi-view graph in the context of a DDI network.

Methodology

This section introduces the proposed DDI prediction approach, which is an end-to-end representation learning model consisting of three sequential and interdependent phases. We will depict the architecture, optimization objective, and training process. Figure 2 illustrates the framework of the proposed MIRACLE method.

Notations and Problem Formulation

Before presenting our proposed model, We summarize the important notations adopted in this paper. We use upper boldface letters for matrices (*e.g.* $\mathbf{A} \in \mathbb{R}^{m \times n}$), boldface letters for vectors (*e.g.* $\mathbf{h} \in \mathbb{R}^d$), normal characters for scalars (*e.g.* d_g for the dimension of molecule-level embedding, d_h for the dimension of atom-level embedding), and calligraphic for sets (*e.g.* \mathcal{G}).

Suppose that we have a graph \mathcal{G} which is presented by $\mathcal{G} = \{\mathcal{V}, \mathcal{E}\}$ where \mathcal{V} is the set of vertices and \mathcal{E} is the set of edges. We denote the i th atom as $v_i \in \mathcal{V}$ and the chemical bond connecting the i th and j th atoms as $e_{ij} \in \mathcal{E}$.

Problem statement. The DDI prediction task can be defined as a link prediction problem on graph. Given g drug molecular graphs $\mathcal{G} := \{G^{(i)}\}_{i=1}^g$ and DDI network $\mathcal{N} = (\mathcal{G}, \mathcal{L})$ where \mathcal{L} denotes the interaction links, the task link prediction is, for the network \mathcal{N} , predicting the existence of missing links.

Bond-aware Message Passing Network with Attentive Pooling

We equip our model with propagation-based message passing layers according to simple chemistry knowledge and a graph aggregation layer with attentive pooling (Vaswani et

al. 2017) to generate a graph-level representation. The message passing process can be introduced in two successive phases. The first phase can be described using the following message function:

$$\tilde{\mathbf{h}}_i^{(1)} = \sum_{j \in \mathcal{C}(i)} \mathbf{W}_{c_{ij}}^{(1)} \mathbf{h}_j^{(1-1)} \quad (1)$$

where $\mathbf{W}_{c_{ij}}^{(1)} \in \mathbb{R}^{d_h \times d_h}$ is a matrix of trainable parameters shared by the same type of chemical bond c_{ij} at the l th layer, $\tilde{\mathbf{h}}_i^{(1)}$ represents the candidate hidden state at the l th layer for node v_i , $\mathbf{h}_j^{(1-1)} \in \mathbb{R}^{d_h}$ represents the hidden state at the $(l-1)$ th layer for the neighbor node v_j , and $\mathcal{C}(i)$ denotes the neighbor nodes of the center node v_i .

The equation(1) shows that the node information corresponding to the same type of chemical bond share parameters during the affine transformation. The chemical interpretability for this message function is straightforward: neighboring nodes connected by the same type of chemical bond have similar effects, and vice versa.

Given $\hat{\mathbf{h}}_i^{(1)} = [\mathbf{h}_i^{(1-1)}; \tilde{\mathbf{h}}_i^{(1)}]$ where $[;]$ denotes the concatenation operation, for the second phase, inspired by Srivastava, Greff, and Schmidhuber(2015), we additionally define three non-linear transforms $F(\mathbf{W}_f, \hat{\mathbf{h}}_i^{(1)})$, $T(\mathbf{W}_t, \hat{\mathbf{h}}_i^{(1)})$, and $C(\mathbf{W}_c, \hat{\mathbf{h}}_i^{(1)})$. Thus, this process can be described as the following update function:

$$\begin{aligned} \mathbf{h}_i^{(1)} = & T(\mathbf{W}_t, \hat{\mathbf{h}}_i^{(1)}) \odot F(\mathbf{W}_f, \hat{\mathbf{h}}_i^{(1)}) \\ & + C(\mathbf{W}_c, \hat{\mathbf{h}}_i^{(1)}) \odot \mathbf{h}_i^{(1-1)} \end{aligned} \quad (2)$$

where $\mathbf{h}_i^{(1)}$ represents the hidden state at the l th layer for node v_i , and \odot denotes the element-wise product. We refer to F as the *fuse* gate, T as the *transform* gate, and C as the *carry* gate, since they express how much of the hidden state is produced by transforming the fusion of the candidate and previous hidden state and carrying it, respectively. We can take both the influence on the concentrated center node exerted by neighboring ones and itself at the previous layer into consideration through this update process.

We stack several message passing layers (L in total) to learn the hidden representation for every node/atom v in a molecular graph \mathcal{G} and obtain the final hidden states for each atom at the last message passing layer. To make predictions with drug representations, we need to generate an embedding vector for each molecular graph. Therefore, we apply a simple but efficient attentive readout layer inspired by Li et al.(2015) as follows:

$$\mathbf{a}_i = \tanh(\mathbf{W}_a[\mathbf{h}_i^{(0)}; \mathbf{h}_i^{(L)}] + \mathbf{b}_a) \quad (3)$$

$$\mathbf{g} = \sum_{v_i \in \mathcal{V}} \mathbf{a}_i \odot (\mathbf{W}_o \mathbf{h}_i^{(L)} + \mathbf{b}_o) \quad (4)$$

where $[;]$ denotes the concatenation operation, $\tanh(\cdot)$ denotes the tanh activation function, attention score $\mathbf{a}_i \in \mathbb{R}^{d_g}$ denotes the importance score of the atom v_i , \odot denotes the element-wise product, and $\mathbf{g} \in \mathbb{R}^{d_g}$ is the obtained embedding vector for the molecular graph. Stacking the embedding vectors of drugs over given dataset, we get the inter-view embedding matrix $\mathbf{G} \in \mathbb{R}^{n \times d_g}$. It should be noted that all of the parameters are shared across all the atoms.

GCN for Integrating Multi-view Network Information

We establish an encoder to integrate the multi-view network information. In the following, we utilize a multi-layer GCN(M in total) to smooth each node's features over the graph's topology. In this context, we refer to the node's features as low-dimensional representations of drugs learned from the previous message passing network and the graph's topology as the interaction relationship inside the DDI network.

Assumed the number of drugs in the DDI network is denoted by n , formally, we are given the adjacency matrix of DDI network $\mathbf{A} \in \mathbb{R}^{n \times n}$ and the attribute matrix $\mathbf{G} \in \mathbb{R}^{n \times d_g}$ of the DDI network \mathcal{N} as inputs. Before the graph convolution operation, we normalized the adjacency matrix \mathbf{A} :

$$\hat{\mathbf{A}} = \tilde{\mathbf{K}}^{-\frac{1}{2}} (\mathbf{A} + \mathbf{I}_n) \tilde{\mathbf{K}}^{-\frac{1}{2}} \quad (5)$$

where \mathbf{I}_n represents the identity matrix and $\tilde{\mathbf{K}}_{ii} = \sum_j (\mathbf{A} + \mathbf{I}_n)_{ij}$. Then we apply the GCN encoder framework as follows:

$$\begin{aligned} \mathbf{D}^{(1)} &= U(\mathbf{A}, \mathbf{G}, \mathbf{W}_u^{(0)}, \mathbf{W}_u^{(1)}) \\ &= \hat{\mathbf{A}} \text{ReLU}(\hat{\mathbf{A}} \mathbf{G} \mathbf{W}_u^{(0)}) \mathbf{W}_u^{(1)} \end{aligned} \quad (6)$$

where $\mathbf{W}_u^{(0)} \in \mathbb{R}^{d_u^{(0)} \times d_u^{(1)}}$ and $\mathbf{W}_u^{(1)} \in \mathbb{R}^{d_u^{(1)} \times d_u^{(2)}}$ are two weight parameters at the 0th and 1th layer of the GCN encoder, respectively. The second dimension of the weight parameter at the last layer of the GCN encoder is set1 to d_g . Through the GCN encoder, then we get the intra-view embedding matrix $\mathbf{D} \in \mathbb{R}^{n \times d_g}$ for drugs in the DDI network \mathcal{N} .

Contrastive Learning of Drug Representation

The inter-view drug embeddings are learned directly from molecular graphs, including raw attributes and structural information. Specifically, the representations may contain multiple functional groups' information inside a molecule,

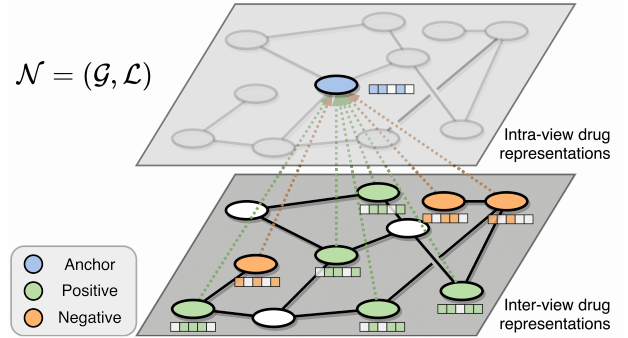


Figure 3: The proposed contrastive learning framework.

different local connectivity constructed by various combinations of the same atoms and bonds, etc. Such information has a significant influence on interaction predictions. However, after graph convolutions, the inter-view features are smoothed over the whole DDI network topology and become blurred. Therefore, it is necessary to balance multi-view information in the drug embeddings. We propose a novel graph contrastive learning framework to handle these issues.

Figure 3 illustrates the proposed graph contrastive learning component. In MIRACLE, we naturally have two different graph views in the multi-view graph setting to learn drug representations by maximizing the agreement between inter-view and intra-view embeddings. We define our mutual information(MI) estimator on inter- and intra-view pairs, maximizing the estimated MI over the given dataset \mathcal{N} . To be specific, for each drug i , fixing itself as an anchor A , we get a set of positive samples \mathbb{P} which is made up of itself and its k -order neighboring nodes, and a set of negative samples \mathbb{N} from nodes not in its k -hop neighbors. Considering the assumption that representations of drugs that interact with the same drug may contain similar information, we usually set $k = 1$. Then, we generate each positive pair (A, P) where $P \in \mathbb{P}$ and negative pair (A, N) where $N \in \mathbb{N}$. After iterations, we can obtain all possible positive pairs and negative pairs. Afterward, we employ a contrastive objective that enforces the intra-view representation of the anchor A agree with the inter-view representations of the positive samples and can be distinguished from the inter-view representations of the negative samples. The contrastive objective is formulated as follows:

$$\hat{\omega}, \hat{\phi}, \hat{\psi} = \underset{\omega, \phi, \psi}{\operatorname{argmax}} \sum_{i \in \mathcal{G}} \frac{1}{\tilde{C}(i)} \sum_{j \in \mathcal{C}(i) \cap \{i\}} \hat{\mathcal{I}}_{\omega, \phi, \psi}(\mathbf{g}_j^\phi; \mathbf{d}_i^\psi) \quad (7)$$

where $\tilde{C}(i) := |\mathcal{C}(i)| + 1$, ϕ and ψ denote the set of parameters of the BAMPN and GCN encoder, respectively, $\hat{\mathcal{I}}_{\omega, \phi, \psi}$ is the mutual information estimator modeled by discriminator \mathcal{T}_ω and parameterized by a neural network with parameters ω . As stated in Hjelm et al.(2018), contrastive learning-based methods concentrate primarily on the maximization of mutual information instead of its precise value. Therefore, we use the Jensen-Shannon MI estimator (following

the formulation of Nowozin, Cseke, and Tomioka(2016)),

$$\begin{aligned}\hat{\mathcal{L}}_{\omega, \phi, \psi}(\mathbf{g}_j^\phi; \mathbf{d}_i^\psi) := & \mathbb{E}_{\mathbb{D}}[-sp(-\mathcal{T}_{\omega, \phi, \psi}(\mathbf{g}_j^\phi(\mathbf{x}); \mathbf{d}_i^\psi(\mathbf{x})))] \\ & - \mathbb{E}_{\tilde{\mathbb{D}} \times \tilde{\mathbb{D}}} [sp(\mathcal{T}_{\omega, \phi, \psi}(\mathbf{g}_j^\phi(\mathbf{x}'); \mathbf{d}_i^\psi(\mathbf{x}')))]\end{aligned}\quad (8)$$

where x is an input sample, x' is an input sample from $\tilde{\mathbb{D}} = \mathbb{D}$, \mathbb{D} denotes an empirical probability distribution, and $sp(\cdot)$ is the softplus function. It should be noted that we generate negative samples using all possible combinations of inter/intra-view embeddings across all drugs in a batch. Since \mathbf{d}_i^ψ is encouraged to have high MI with samples containing information at both views, this favors encoding aspects of the data shared across different samples and views.

Drug-drug Interaction Prediction

For each interaction link $l_{ij} \in \mathcal{L}$, We first compress two drug embedding vectors into an interaction link embedding vector. Then we apply a two-layer fully-connected neural network to make the final prediction:

$$\mathbf{p} = \sigma(\mathbf{W}_P \text{ReLU}(\mathbf{W}_1(\mathbf{d}_i \odot \mathbf{d}_j) + \mathbf{b}_1) + \mathbf{b}_P) \quad (9)$$

where $\mathbf{p} \in \mathbb{R}^k$ and \odot denotes the element-wise product. If the aim is to predict the occurrence of DDIs, k is 2, while k equals to the total number of DDI types if our target is to predict the specific DDI type(s).

Besides, we design an auxiliary interaction predictor using the inter-view drug embeddings. The prediction of the inter-view interaction predictor is denoted as $\mathbf{r} \in \mathbb{R}^k$. Optimizing the inter-view interaction prediction results can help the supervised information directly flow into previous network layers. The model learns the commonality between different views through a disagreement loss, which will be discussed below. It should be noted that we only use \mathbf{p} for the final DDI prediction.

Training Both predictors' primary goal is to minimize the supervised loss, which measures the distance between the predictions and the true labels. Another goal is to minimize a disagreement loss, which measures the distance between two predictors' predictions. The purpose of minimizing this disagreement loss is to enforce the model to pay more attention to the commonality between two different views and consistency between two predictors.

Formally, we formulate the supervised loss for the labeled interaction links and the disagreement loss for the unlabeled interaction links:

$$\mathcal{L}_s = \sum_{l_i \in \mathcal{L}_l} (\mathcal{C}(\mathbf{r}_i, \mathbf{y}_i) + \mathcal{C}(\mathbf{p}_i, \mathbf{y}_i)) \quad (10)$$

$$\mathcal{L}_d = \sum_{l_j \in \mathcal{L}_u} \mathcal{K}(\mathbf{p}_j || \mathbf{r}_j) \quad (11)$$

where y_i is the true label of l_i , \mathcal{L}_l and \mathcal{L}_u denote the labeled and unlabeled links in \mathcal{L} respectively, $\mathcal{C}(\cdot, \cdot)$ is the cross-entropy loss function and $\mathcal{K}(\cdot || \cdot)$ is the Kullback-Leibler divergence.

With contrastive loss \mathcal{L}_c , supervised loss \mathcal{L}_s and disagreement loss \mathcal{L}_d , the objective function of our model is,

$$\mathcal{L} = \mathcal{L}_s + \alpha \mathcal{L}_c + \beta \mathcal{L}_d \quad (12)$$

where α and β are hyper-parameters for the trade-off for different loss components. With the objective function, we use the back-propagation algorithm to find the best solution for the trainable parameters ω, ϕ, ψ .

Experiments

We conduct experiments on three benchmark datasets, i.e., *ZhangDDI*(Zhang et al. 2017) with all types of drug features, *ChCh-Miner*(Marinka Zitnik and Leskovec 2018) with few labeled DDI links and *DeepDDI*(Ryu, Kim, and Lee 2018) with missing drug features to verify our proposed method's effectiveness in different scenarios. The comparing methods are summarized in table 1.

Dataset Description

We evaluate the proposed method on three benchmark datasets, i.e., *ZhangDDI*¹, *ChCh-Miner*² and *DeepDDI*³ with different scales for verifying the scalability and robustness of our model. These three datasets are small-scale, medium-scale, and large-scale, respectively. The *ZhangDDI* dataset contains a relatively small number of drugs where all the fingerprints are available for all drugs. However, for *DeepDDI*, the large-scale one, many fingerprints are missing in most drugs. For the *ChCh-Miner* dataset, although it has almost three times the number of drugs in the *ZhangDDI* dataset, it only has the same number of labeled DDI links. The statistics of datasets are summarized as follows:

- *ZhangDDI*(Zhang et al. 2017): This dataset contains 548 drugs and 48,548 pairwise DDIs and multiple types of similarity information about these drug pairs. We remove the data items that cannot be converted into graphs from SMILES strings in our preprocessing.
- *ChCh-Miner*(Marinka Zitnik and Leskovec 2018): This dataset contains 1,514 drugs and 48,514 DDI links without similarity-based fingerprints and polypharmacy side-effect information of each drug pair. We remove the data items that cannot be converted into graphs from SMILES strings in our preprocessing.
- *DeepDDI*(Ryu, Kim, and Lee 2018): This dataset contains 192,284 DDIs from 191,878 drug pairs and their polypharmacy side-effect information extracted from DrugBank(Wishart et al. 2018). We also remove the data items that cannot be converted into graphs from SMILES strings in our preprocessing.

¹<https://github.com/zw9977129/drug-drug-interaction/tree/master/dataset>

²<http://snap.stanford.edu/biodata/datasets/10001/10001-ChCh-Miner.html>

³<https://zenodo.org/record/1205795>

Comparing Methods

To demonstrate the superiority of our proposed model, we implement many baseline approaches to compare their performance. The compared baselines cover similarity-based methods and graph-based methods:

- **Nearest Neighbor**(Vilar et al. 2012): Vilar and his team used known interactions between drugs and similarity derived from substructure to conduct DDI prediction. We refer to the model as **NN** for simplicity.
- **Label Propagation**: Zhang et al.(2015) utilized the label propagation(LP) algorithm to build three similarity-based predictive models. The similarity is calculated based on the substructure, side effect, and off-label side effect, respectively. We refer to the three models as **LP-Sub**, **LP-SE** and **LP-OSE**, respectively.
- **Multi-Feature Ensemble**: Zhang et al.(2017) employed neighbor recommendation(NR) algorithm, label propagation(LP) algorithm, and matrix disturbs (MD) algorithm to build a hybrid ensemble model. The ensemble model exploited different aspects of drugs. We name the model as **Ens**.
- **SSP-MLP**: Ryu, Kim, and Lee(2018) applied the combination of precomputed low dimensional Structural Similarity Profile(SSP) and Multi-layer Perceptron to conduct the classification. We will refer to the model as **SSP-MLP**.
- **GCN**: Kipf and Welling(2016) used a graph convolutional network(GCN) for semi-supervised node classification tasks. We applied **GCN** to encode drug molecular graphs and learn their representations to make predictions as a baseline.
- **GIN**: Xu et al.(2018) proposed a graph isomorphism network (GIN) to learn molecules’ representations in various single-body property prediction tasks. We used **GIN** to encode drug molecular graphs and learn their representations to make predictions as a baseline.
- **Attentive Graph Autoencoder**: Ma et al.(2018) designed an attentive mechanism to integrate multiple drug similarity views, which will be fed into a graph autoencoder to learn the embedding vector for each drug. We referred to the model as **AttGA** and made predictions based on the learned drug representations pairwise as a baseline.
- **GAT**: Veličković et al.(2017) utilized a graph attention network(GAT) to learn node embeddings by a well-designed attention mechanism on the graph. We used **GAT** to obtain drug embeddings on the DDI network for link prediction tasks.
- **SEAL-CI**: Li et al.(2019) firstly applied a hierarchical graph representation learning framework in semi-supervised graph classification tasks. We named this model as **SEAL-CI** and used the model to learn drug representations for DDI link prediction as a baseline.
- **NFP-GCN**: Duvenaud et al.(2015) is the first graph convolution operator, which is specific to molecules. We named the model as **NFP-GCN**. We changed our bond-aware message passing network into NFP to be a baseline.

Evaluation Metrics and Experimental Settings

We divide the entire interaction samples into a training set and a test set with a ratio of 4 : 1, and randomly select 1/4 of the training dataset as a validation dataset. We set each parameter group’s learning rate using an exponentially decaying schedule with the initial learning rate 0.0001 and multiplicative factor 0.96. For the proposed model’s hyperparameters, we set the dimension of the hidden state of atoms and drugs as 256. The total number of the bond-aware message passing neural networks and the GCN encoder is 3. The coefficients α and β in objective functions are set to 100 and 0.8, respectively, making the model achieve the best performance. To further regularise the model, dropout(Srivastava et al. 2014) with $p = 0.3$ is applied to every intermediate layer’s output.

We implement our proposed model with Pytorch 1.4.0(Paszke et al. 2019) and Pytorch-geometric 1.4.2(Fey and Lenssen 2019). Models are trained using Adam(Kingma and Ba 2014) optimizer. The model is initialized using Xavier(Glorot and Bengio 2010) initialization. We choose three metrics to evaluate our proposed model’s effectiveness: *area under the ROC curve(AUROC)*, *area under the PRC curve(AUPRC)*, and *F1*. For multi-label classification, we choose the *macro* averages. We report the mean and standard deviation of these metrics over ten repetitions.

Comparison on ZhangDDI Table 2 compares our MIRACLE against baselines on *ZhangDDI*, where almost all types of drug features can be used for DDI prediction. The best results are highlighted in boldface. The performance of baselines utilizing similarity-based fingerprints like **NN**, **LP**, and **SSP-MLP** are relatively poor, which only incorporate one important feature. However, contrary to them, **Ens** obtains better results because of the combination of three distinct models utilizing eight types of drug feature similarities coupling with another six types of topological ones, demonstrating the importance of integrating information from multiple sources like similarity-based fingerprints and topological features.

Some graph-based methods perform worse than the models mentioned above because they only rely on single view information. **GCN** and **GIN** encode drug molecular graphs and make predictions pairwise based on the obtained drug molecule representations. **AttGA** and **GAT** directly learn drug representations from DDI interaction relationships and make predictions. **AttGA** obtains drug representations according to different similarity matrices of the DDI network, which achieves better performance than **GAT**, which only considers the DDI network’s link existence.

The compared baselines in the multi-view graph settings like **SEAL-CI** and **NFP-GCN** outperform other baselines, demonstrating the integration of multi-view graph can improve the performance of models significantly. However, their performance is still inferior to that of **MIRACLE**. Compared with them, MIRACLE further considers the importance of the message passing mechanism in terms of chemical bonds inside drug molecular graphs and the balance between multi-view graph information, which can learn more comprehensive drug representations.

Table 1: Comparison of baseline methods.

Algorithm	Model Type	Inter-view	Intra-view	Feature Type
NN(Vilar et al. 2012)	similarity-based	N/A	N/A	similarity-based fingerprint
LP(Zhang et al. 2015)	similarity-based	N/A	N/A	similarity-based fingerprint
Ens(Zhang et al. 2017)	similarity-based	N/A	N/A	similarity-based fingerprint
SSP-MLP(Ryu, Kim, and Lee 2018)	similarity-based	N/A	N/A	similarity-based fingerprint
GCN(Kipf and Welling 2016)	inter-view	GCN	N/A	Molecular Graph
GIN(Xu et al. 2018)	inter-view	GIN	N/A	Molecular Graph
AttGA(Ma et al. 2018)	intra-view	N/A	AttGA	Interaction Relationship
GAT(Ma et al. 2018)	intra-view	N/A	GAT	Interaction Relationship
SEAL-CI(Li et al. 2019)	multi-view	GCN	GCN	Molecular Graph & Interaction Relationship
NFP-GCN(Duvenaud et al. 2015)	multi-view	NFP	GCN	Molecular Graph & Interaction Relationship
MIRACLE(Ours)	multi-view	BAMPN	GCN	Molecular Graph & Interaction Relationship

Table 2: Comparative evaluation results on *ZhangDDI*

Algorithm	Performance		
	AUROC	AUPRC	F1
NN	67.81 ± 0.25	52.61 ± 0.27	49.84 ± 0.43
LP-Sub	93.39 ± 0.13	89.15 ± 0.13	79.61 ± 0.16
LP-SE	93.48 ± 0.25	89.61 ± 0.19	79.83 ± 0.61
LP-OSE	93.50 ± 0.24	90.31 ± 0.82	80.41 ± 0.51
Ens	95.20 ± 0.14	92.51 ± 0.15	85.41 ± 0.16
SSP-MLP	92.51 ± 0.15	88.51 ± 0.66	80.69 ± 0.81
GCN	91.91 ± 0.62	88.73 ± 0.84	81.61 ± 0.39
GIN	81.45 ± 0.26	77.16 ± 0.16	64.15 ± 0.16
AttGA	92.84 ± 0.61	90.21 ± 0.19	70.96 ± 0.39
GAT	91.49 ± 0.29	90.69 ± 0.10	80.93 ± 0.25
SEAL-CI	92.93 ± 0.19	92.82 ± 0.17	84.74 ± 0.17
NFP-GCN	93.22 ± 0.09	93.07 ± 0.46	85.29 ± 0.38
MIRACLE	98.95 ± 0.15	98.17 ± 0.06	93.20 ± 0.27

Whereas in **SEAL-CI** and **NFP-GCN**, they model the multi-view graphs with information equilibrium between different views ignored. Besides, **MIRACLE** adopts the attentive mechanism to generate an inter-view drug representation that automatically selects the most significant atoms that form meaningful functional groups in DDI reactions and neglect noisy, meaningless substructures.

Comparison on ChCh-Miner In this part of the experiment, we aim to evaluate **MIRACLE** with few labeled DDI links. We only compare **MIRACLE** with graph-based baselines because *ChCh-Miner* lacks similarity-based fingerprints for drug pairs. For the same reason, **AttGA** is ignored. Table 3 shows the results.

Obviously, methods taking multi-view information into consideration like **SEAL-CI** and **NFP-GCN** outperform baselines that only use single-view information. However, **MIRACLE** achieves the best performance and substantially exceeds baselines, demonstrating the superiority of our proposed method on datasets with few labeled data.

Comparison on DeepDDI To verify **MIRACLE**'s scalability, we also conduct experiments on *DeepDDI*, which is large-scale and has multiple DDI information types. Table 4 compares **MIRACLE** with baselines who are applicable in this dataset. We also ignore experimental results obtained by **GIN** and **NFP-GCN** because of the worse performance and the space limitation.

Table 3: Comparative evaluation results on *ChCh-Miner*

Algorithm	Performance		
	AUROC	AUPRC	F1
GCN	82.84 ± 0.61	84.27 ± 0.66	70.54 ± 0.87
GIN	70.32 ± 0.87	72.41 ± 0.63	65.54 ± 0.97
GAT	85.84 ± 0.23	88.14 ± 0.25	76.51 ± 0.38
SEAL-CI	90.93 ± 0.19	89.38 ± 0.39	84.74 ± 0.48
NFP-GCN	92.12 ± 0.09	93.07 ± 0.69	85.41 ± 0.18
MIRACLE	96.15 ± 0.29	95.57 ± 0.19	92.26 ± 0.09

Table 4: Comparative evaluation results on *DeepDDI*

Algorithm	Performance		
	AUROC	AUPRC	F1
NN	81.81 ± 0.37	80.82 ± 0.20	71.37 ± 0.18
SSP-MLP	92.28 ± 0.18	90.27 ± 0.28	79.71 ± 0.16
GCN	85.53 ± 0.17	83.27 ± 0.31	72.18 ± 0.22
GAT	84.84 ± 0.23	81.14 ± 0.25	73.51 ± 0.38
SEAL-CI	92.83 ± 0.19	90.44 ± 0.39	80.70 ± 0.48
MIRACLE	95.51 ± 0.27	92.34 ± 0.17	83.60 ± 0.33

MLP-SSP substantially outperforms **NN** for the former is based on deep neural networks. **GCN** achieves better performance than **GAT**, which further demonstrates the inter-view information plays a vital role in DDI predictions. **SEAL-CI** is second to the proposed method among the baselines proving the superiority of the multi-view graph framework. **MIRACLE** significantly outperformed other baseline methods in terms of all three metrics.

Conclusion

To better integrate the rich multi-view graph information in the DDI network, we propose **MIRACLE** for the DDI prediction task in this paper. **MIRACLE** learns drug embeddings from a multi-view graph perspective by designing an end-to-end framework that consists of a bond-aware message passing network and a GCN encoder. Then, a novel contrastive learning-based strategy has been proposed to balance information from different views. Also, we design two predictors from both views to fully exploit the available information. Through extensive experiments on various real-life datasets, we have demonstrated that the proposed **MIRACLE** is both effective and efficient.

References

- [Duvenaud et al. 2015] Duvenaud, D. K.; Maclaurin, D.; Iparraguirre, J.; Bombarell, R.; Hirzel, T.; Aspuru-Guzik, A.; and Adams, R. P. 2015. Convolutional networks on graphs for learning molecular fingerprints. In *Advances in neural information processing systems*, 2224–2232.
- [Fey and Lenssen 2019] Fey, M., and Lenssen, J. E. 2019. Fast graph representation learning with pytorch geometric. *arXiv preprint arXiv:1903.02428*.
- [Glorot and Bengio 2010] Glorot, X., and Bengio, Y. 2010. Understanding the difficulty of training deep feedforward neural networks. In *Proceedings of the thirteenth international conference on artificial intelligence and statistics*, 249–256.
- [Hjelm et al. 2018] Hjelm, R. D.; Fedorov, A.; Lavoie-Marchildon, S.; Grewal, K.; Bachman, P.; Trischler, A.; and Bengio, Y. 2018. Learning deep representations by mutual information estimation and maximization. *arXiv preprint arXiv:1808.06670*.
- [Kingma and Ba 2014] Kingma, D. P., and Ba, J. 2014. Adam: A method for stochastic optimization. *arXiv preprint arXiv:1412.6980*.
- [Kipf and Welling 2016] Kipf, T. N., and Welling, M. 2016. Semi-supervised classification with graph convolutional networks. *arXiv preprint arXiv:1609.02907*.
- [Li et al. 2015] Li, Y.; Tarlow, D.; Brockschmidt, M.; and Zemel, R. 2015. Gated graph sequence neural networks. *arXiv preprint arXiv:1511.05493*.
- [Li et al. 2019] Li, J.; Rong, Y.; Cheng, H.; Meng, H.; Huang, W.; and Huang, J. 2019. Semi-supervised graph classification: A hierarchical graph perspective. In *The World Wide Web Conference*, 972–982.
- [Ma et al. 2018] Ma, T.; Xiao, C.; Zhou, J.; and Wang, F. 2018. Drug similarity integration through attentive multi-view graph auto-encoders. *arXiv preprint arXiv:1804.10850*.
- [Marinka Zitnik and Leskovec 2018] Marinka Zitnik, Rok Sosič, S. M., and Leskovec, J. 2018. BioSNAP Datasets: Stanford biomedical network dataset collection. <http://snap.stanford.edu/biodata>.
- [Nowozin, Cseke, and Tomioka 2016] Nowozin, S.; Cseke, B.; and Tomioka, R. 2016. f-gan: Training generative neural samplers using variational divergence minimization. In *Advances in neural information processing systems*, 271–279.
- [Paszke et al. 2019] Paszke, A.; Gross, S.; Massa, F.; Lerer, A.; Bradbury, J.; Chanan, G.; Killeen, T.; Lin, Z.; Gimelshein, N.; Antiga, L.; et al. 2019. Pytorch: An imperative style, high-performance deep learning library. In *Advances in neural information processing systems*, 8026–8037.
- [Ryu, Kim, and Lee 2018] Ryu, J. Y.; Kim, H. U.; and Lee, S. Y. 2018. Deep learning improves prediction of drug-drug and drug-food interactions. *Proceedings of the National Academy of Sciences* 115(18):E4304–E4311.
- [Srivastava et al. 2014] Srivastava, N.; Hinton, G.; Krizhevsky, A.; Sutskever, I.; and Salakhutdinov, R. 2014. Dropout: a simple way to prevent neural networks from overfitting. *The journal of machine learning research* 15(1):1929–1958.
- [Srivastava, Greff, and Schmidhuber 2015] Srivastava, R. K.; Greff, K.; and Schmidhuber, J. 2015. Highway networks. *arXiv preprint arXiv:1505.00387*.
- [Sun et al. 2020] Sun, M.; Zhao, S.; Gilvary, C.; Elemento, O.; Zhou, J.; and Wang, F. 2020. Graph convolutional networks for computational drug development and discovery. *Briefings in bioinformatics* 21(3):919–935.
- [Vaswani et al. 2017] Vaswani, A.; Shazeer, N.; Parmar, N.; Uszkoreit, J.; Jones, L.; Gomez, A. N.; Kaiser, Ł.; and Polosukhin, I. 2017. Attention is all you need. In *Advances in neural information processing systems*, 5998–6008.
- [Veličković et al. 2017] Veličković, P.; Cucurull, G.; Casanova, A.; Romero, A.; Lio, P.; and Bengio, Y. 2017. Graph attention networks. *arXiv preprint arXiv:1710.10903*.
- [Vilar et al. 2012] Vilar, S.; Harpaz, R.; Uriarte, E.; Santana, L.; Rabadan, R.; and Friedman, C. 2012. Drug—drug interaction through molecular structure similarity analysis. *Journal of the American Medical Informatics Association* 19(6):1066–1074.
- [Wishart et al. 2018] Wishart, D. S.; Feunang, Y. D.; Guo, A. C.; Lo, E. J.; Marcu, A.; Grant, J. R.; Sajed, T.; Johnson, D.; Li, C.; Sayeeda, Z.; et al. 2018. Drugbank 5.0: a major update to the drugbank database for 2018. *Nucleic acids research* 46(D1):D1074–D1082.
- [Xin, Xien, and Ji 2020] Xin, C.; Xien, L.; and Ji, W. 2020. Research progress on drug representation learning. *Journal of Tsinghua University (Science and Technology)* 60(2):171–180.
- [Xu et al. 2018] Xu, K.; Hu, W.; Leskovec, J.; and Jegelka, S. 2018. How powerful are graph neural networks? *arXiv preprint arXiv:1810.00826*.
- [Zhang et al. 2015] Zhang, P.; Wang, F.; Hu, J.; and Sorrentino, R. 2015. Label propagation prediction of drug-drug interactions based on clinical side effects. *Scientific reports* 5(1):1–10.
- [Zhang et al. 2017] Zhang, W.; Chen, Y.; Liu, F.; Luo, F.; Tian, G.; and Li, X. 2017. Predicting potential drug-drug interactions by integrating chemical, biological, phenotypic and network data. *BMC bioinformatics* 18(1):18.